

# Optical spectroscopy of Cyg X-1

Petr Hadrava

Astronomical Institute, Academy of Sciences, Boční II 1401,  
CZ-14131 Prague, Czech Republic

## ABSTRACT

The star HDE 226868 known as an optical counterpart of the black hole candidate Cyg X-1 has been observed in  $H_\alpha$  region using spectrograph at Ondřejov 2-m telescope. The orbital parameters are determined from He I-line by means of the author's method of Fourier disentangling. Preliminary results are also presented of disentangling the  $H_\alpha$ -line into a P-Cyg profile of the (optical) primary and an emission profile of the circumstellar matter (and a telluric component).

## 1 INTRODUCTION

The bright X-ray source Cyg X-1 has been identified with the star denoted as HDE 226868, V1357 Cyg or BD+34°3815 etc. An improvement of instrumentation of the Ondřejov 2-m telescope enabled to start with systematic observations of this target of magnitude  $V \simeq 8.9$ ,  $B \simeq 9.6$ . With coordinates  $\alpha_{2000} = 19^h 58^m 21.7^s$ ,  $\delta_{2000} = +35^\circ 12' 6''$  it is well observable from Ondřejov mainly at summer.

It is known to be an interacting binary with period  $P \simeq 5.6d$ . The primary component is a supergiant of spectral type classified as B0 (or O9.7) Iab with temperature  $T_{\text{eff}} = 30400 \pm 500$  K and  $\log g = 3.31 \pm 0.07$ . This primary, which nearly fills its Roche lobe, shows signs of variable strong stellar wind and an overabundance of He and heavier elements (cf. e.g. Karitskaya et al. 2007).

The secondary component invisible in optical radiation is a compact object, most probably a black hole. This companion, or its neighborhood emits a variable X-radiation, which is supposed to originate from an accretion disk fed by the stellar wind from the primary.

The X-radiation switches chaotically between two states. In the low/hard state the total X-ray flux is low and the spectrum is flat, so that the hard tail of X-radiation prevails. In the high/soft state the soft radiation is enhanced more, and consequently the spectrum has a steeper decrease toward the higher energies and hence the radiation is softer in the mean. Some intermediate states may also appear temporarily.

The X-ray flux is anticorrelated with the strength of emission in the  $H_\alpha$ -line of the primary: in the X-low/hard state the  $H_\alpha$  emission is strong, while in the X-high/soft state the  $H_\alpha$  emission is weak.

The aim of the observational campaign at Ondřejov observatory was to improve orbital parameters of the system, to check a possible spectroscopic features connected with the circumstellar matter (either accretion disk around the black hole, gaseous streams or stellar wind) or with a possible third body, and to get line-profiles enabling a quantitative comparison with a model of the atmosphere and stellar wind of the primary. The first part of obtained spectra was provided for a study on Cyg X-1 organized in a wide international collaboration, the results of which should appear in Gies et al. (2007). In the present contribution, results obtained using the author's method of spectra disentangling from the same set of Ondřejov spectra are given. A more detailed study taking into account also recently obtained spectra is in progress.

## 2 OBSERVATIONAL DATA

The set of spectra used here consists of 24 exposures obtained with CCD in the focus of 700mm camera of Coudé spectrograph of the Ondřejov 2-m telescope between April 1st and September 21st 2003. A typical resolution is about  $0.25\text{\AA}$  per pixel. The rough data have been processed by M. Šlechta according to Škoda & Šlechta (2002).

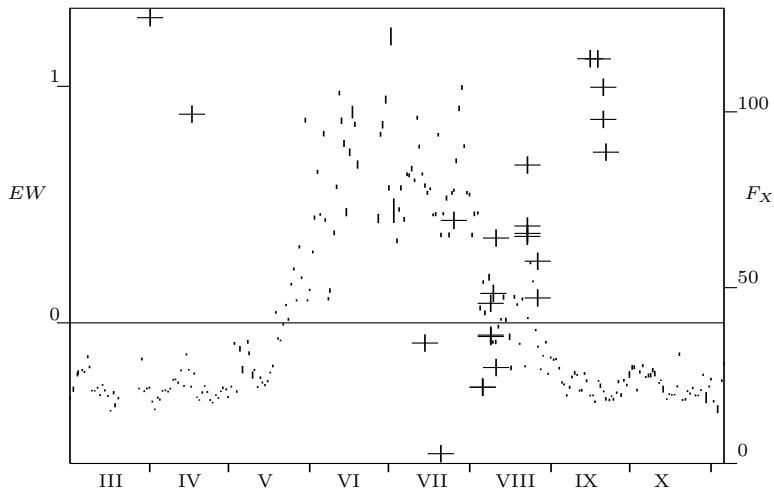


**Figure 1.** The equivalent width of  $H_\alpha$  emission (in  $\text{\AA}$ , crosses) in 2003 and ASM/RXTE one-day averages of sum-band intensity (in counts/s, error-bars)

The observational period covers a transition of Cyg X-1 from the low to high state and back, as it can be seen from the RXTE X-ray light-curve in Fig. 1.

Examples of obtained spectra in both states are given in Fig. 2. It is obvious here that the upper spectrum taken at April before the high-state episode has a strong emission in the whole  $H_\alpha$  line profile, while in August the emission remains in the long-wavelength wing of the line only and the short-wavelength side of the line-profiles reveals an absorption, as it is typical in the P-Cyg line-profiles of stars losing mass via a stellar wind. The strength of the emission can be quantified by the equivalent width of the line, i.e. by an integral across the line of the intensity rectified to the continuum. These values are plotted for each exposure in Fig. 1 which confirms the above mentioned anticorrelation with the X-ray flux.

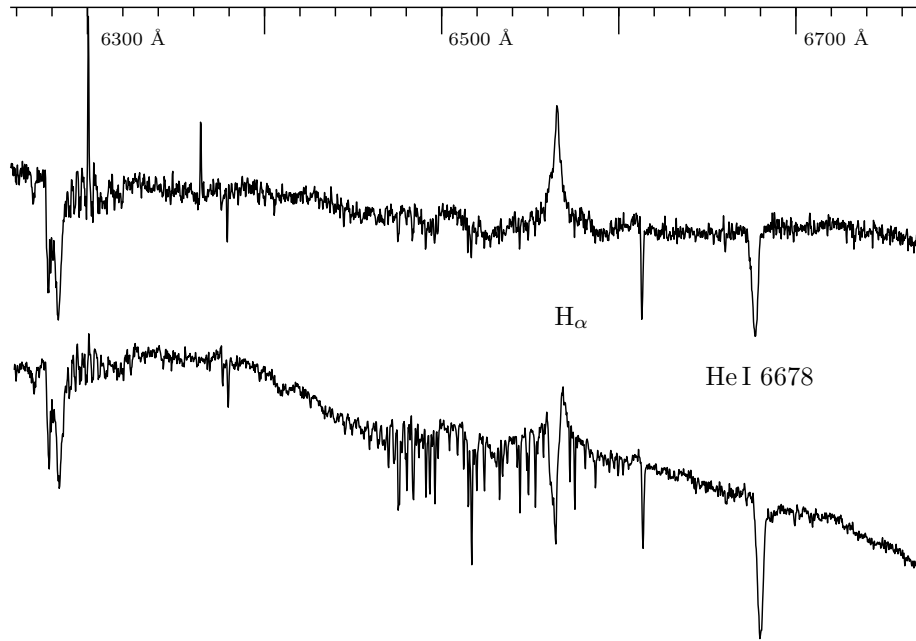


**Figure 2.** Spectra of *Cyg X-1* taken with Ondřejov 2-m telescope on April 1st (upper curve) and August 5th (lower curve) 2003

The He I-line 6678Å is practically free of emission in both states. It means that this line may enable to measure reliably radial velocities of the primary component to get a constraint on the orbital parameters of the system.

### 3 SPECTRA DISENTANGLING

Despite the radial velocities of the He I-line 6678Å could be measured using some standard method, it is advantageous to use the author's method of Fourier spectra disentangling (cf. Hadrava 1994, 1997, 2004), which makes the procedure efficient and provides directly the orbital parameters. The principle of the method (in the

version of 1997 used here) consists in least-squares fitting of all the spectra  $I$  observed at various times  $t$  as a superposition of unknown spectra  $I_j$  of the components in the form

$$I(x, t; p) = \sum_{j=1}^n I_j(x) * s_j(t) \delta(x - v_j(t; p)). \quad (1)$$

Here  $x = c \ln \lambda$  is a logarithmic wavelength,  $v_j$  are instantaneous radial velocities of each component (or logarithms of redshift  $g$ -factors for a general relativistic case),  $s_j$  are factors fitting possibly variable strengths of lines,  $p$  are the orbital parameters to be found. Fourier transform

$$\tilde{I}(y, t; p) = \sum_{j=1}^n \tilde{I}_j(y) \tilde{\Delta}_j(y, t, p) \quad (2)$$

of Eq. (1) separates the solving for  $I_j$  into individual modes; similarly for  $s_j$  one gets a set of linear equations, while  $p$  can be found by some numerical method of optimization (e.g. simplex method in the author's code KOREL). Here  $\Delta_j = s_j \delta(x - v_j)$  in the present calculation, but generally it could also characterize some general broadening function.

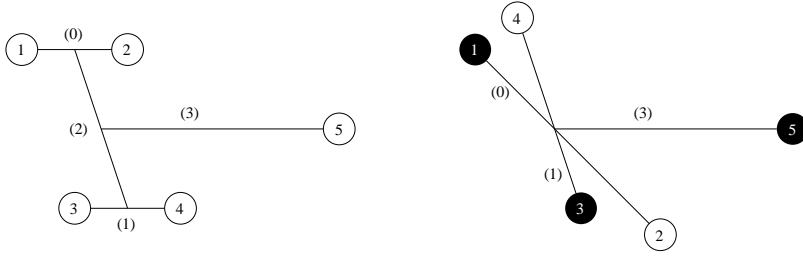


**Figure 3.** Hierarchical structure of a multiple stellar system supposed in KOREL-code (left) and its use for  $H_\alpha$ -line of Cyg X-1 (right)

The method can generally provide intrinsic spectra of  $n$  sources, if more than  $n$  observed spectra taken at different values  $v_j$  are on input. Karas & Kraus (1996) suggested a possibility to disentangle in this way contributions of several spots to a line-profile of an accretion disk. The author's code KOREL should be modified for such a purpose, because it is designed for applications to systems of binary or multiple stars. A hierarchical structure of the system is supposed (cf. Fig. 3, left), in which two pairs of close binaries (denoted 1 + 2 and 3 + 4) are orbiting around their common centre of mass, which may be on an even wider orbit with respect to another component (Nr. 5). To be able to treat simpler systems, spectrum of each component can be switched on or off, and the higher orbits (denoted by numbers in parenthesis in Fig. 3) may be chosen degenerated. At the same time, this model

is general enough to enable solving some more complicated cases, e.g. just like a presence of circumstellar matter in a binary.

As already mentioned, there are seen no traces of the companion or of the circumstellar matter in the He I-line for Cyg X-1. Consequently, one could take the extremally simple case  $n = 1$  of the disentangling (with only the component 1 and orbit (0) switched on – cf. Fig. 3, right) for the spectral region around 6678Å. However, because some weak telluric lines are also present in this region,  $n = 2$  was used instead, with the component 5 corresponding to the telluric lines and orbit (3) to the annual motion. Results of the disentangling are shown on Fig. 4. In the upper part of this standard output from the KOREL-code, we can see superimposed the 24 observed line-profiles (rectified to the continuum) and their reconstructions from the disentangled line-profiles, which are plotted as the two bottom curves. The disentangled values of orbital parameters (the epoch and the amplitude of the radial-velocity curve) are given in Tab. 1.

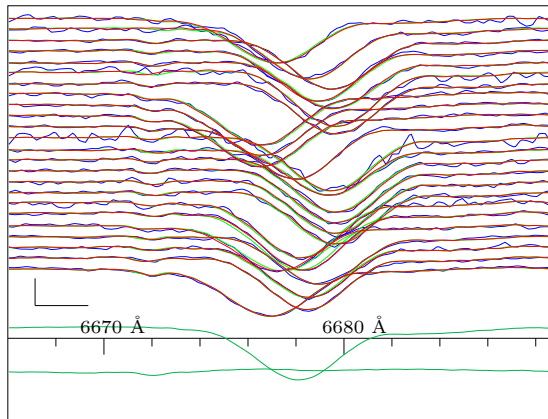


**Figure 4.** Disentangled line He I 6678 Å

#### 4 DOPPLER MAPPING AND DISENTANGLING OF CIRCUMSTELLAR MATTER

Unlike the He I-line, the  $H_\alpha$  shows the above mentioned irregular emission, revealing a presence of strongly variable circumstellar matter in the system. The variability of line-profile of the emission component, which is frequent in many emission-line systems, obviously violates the assumption on constancy of component spectra  $I_j$  in Eq. (1) and makes the use of disentangling for such systems questionable. On the other hand, one can always try, if a violation of underlying assumptions is not an effect of second order, and if a mean behaviour of the system cannot be approximated neglecting this effect, or if the effect cannot be modelled as some additional perturbation.

Line	He I	H $_{\alpha}$	H $_{\alpha}$ – wind
Period		5.599829 d	
Periastron epoch	52872.83	52873.01	52875.41
Eccentricity		0.0	
Periastron long.		-90°	
K $_1$ [km/s]	71.94	71.26	60.78

**Table 1.** Disentangled orbital parameters of Cyg X-1

Several attempts have been done by the author to fit discrepancies between observed spectra of different binaries with circumstellar matter (e.g. Be-stars or algols) and their reconstructions from disentangled spectra. The method consists in fixing the period of orbit (1) equal to that of orbit (0) but converging either epochs or periastron longitudes of both orbits together with the radial-velocity amplitudes ( $K$ ) as independent quantities. If the component 1 and 2 correspond to the primary and secondary star, the component 3 may also be switched on, to correspond to (either emission or absorption) features of the circumstellar matter. The amplitude and phase-shift of this component are then correspond to the absolute value and orientation of the superposition of the orbital and intrinsic velocity of the circumstellar matter with respect to the center of mass of the system. In principle, up to five component spectra corresponding to different features corotating in the orbital plane of a binary may be treated using KOREL, if the periods of all four orbits are fixed equal. Such a disentangling always improved formally the fit, but usually it did not provide a fully satisfactory explanation of a long-lasting series of line-profiles. This may be explained by variations of the motion and emissivity of the circumstellar matter on time-scales shorter than the orbital period.

Sowers et al. (1998) used the method of Doppler mapping to interpret the line-profiles of the H $_{\alpha}$  line of Cyg X-1. They found a good agreement with observations if an emission source attributed to a focused stellar wind is involved. Recently Jingzhi Yan (2007) suggested to disentangle this focused stellar wind and the primary component from the H $_{\alpha}$  line of Cyg X-1. The preliminary results reported here are obtained by switching on the components 1, 3 and 5 for the primary, the focused wind and telluric water-vapor lines (which are quite strong here), resp. The period of orbit (1) is set equal to that of orbit (0), orbit (3) is the annual motion and orbit (2) is degenerated (cf. Fig. 3, right).

The results are shown in Fig. 5 and Tab. 1. The profiles reconstructed from the disentangled components are again superimposed on the observed 24 line-profiles plotted in the chronological order from the top. The agreement of these curves is surprisingly better than the one obtained for some other interacting binaries with much less pronounced variability. The agreement is a bit worse for the first two exposures taken before the X-high episode, also compared to the last exposures, where X-emission was low again and H $_{\alpha}$  emission high (cf. Fig. 4), but still with the P-Cyg profile. The mean line-profile of the primary has a P-Cyg shape, the component attributed to the focused stellar wind is a broad emission. The disen-

tangled spectrum of telluric lines is partly contaminated with the  $H_\alpha$  emission, but again much less than for many other emission-line binaries. Both the primary and wind components are varying in strength, but the analysis of this variability is postponed to a next study based on more spectra disentangled with constrained telluric component as described by Hadrava (2006).

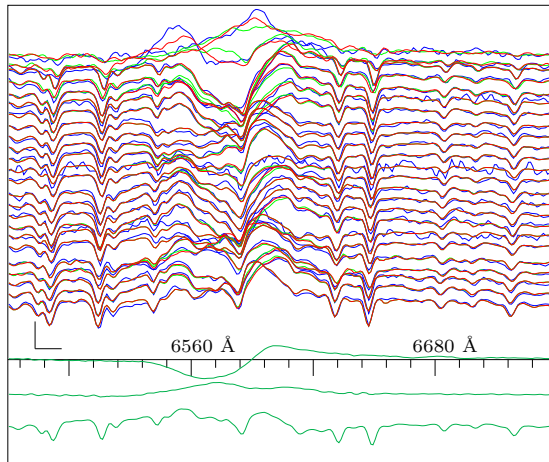


**Figure 5.** Disentangled  $H_\alpha$ -line

The orbital parameters for the primary disentangled from  $H_\alpha$  are in good agreement with those obtained from He-line here as well as in other studies. The radial-velocity amplitude  $K_{wind} = 60.78 \text{ km s}^{-1}$  and the phase shift  $\phi_0 = 0.46$  (with respect to the He-line) of the wind component is not in a complete agreement with results given in text of Sowers et al. (1998, p. 428) who obtained  $K_{wind} = 68 \text{ km s}^{-1}$  and  $\phi_0 = 0.86$  using the tomographic method. Such a disagreement is not surprising, because in spite of some similarities, both methods are different, particularly in taking into account the line-strength variability or the telluric lines. Also the long-term stability of the focused-wind component should be tested by additional spectra. However, the present results indicate, that the velocity-distribution of this component does not vary substantially before and during the episode of high X-ray state.

## ACKNOWLEDGEMENTS

This work has been done in the framework of the Center for Theoretical Astrophysics (ref. LC06014) with a support of grant GACR 202/06/0041. It is based on observational data obtained using Ondřejov 2-m telescope and ASM at RXTE satellite. The work of teams at both these instruments is highly appreciated.

**REFERENCES**

- [1] Gies D.R., Bolton C.T., Blake M., Caballero-Nieves S.M., Crenshaw D.M., Hadrava P., Herrero A., Hillwig T.C., Howell S.B., Huang W., Kaper L., Koubský P., McSwain M.V., Melymuk L. (2007), “Stellar wind variations during the X-ray high and low states of Cygnus X-1”, *ApJ*, submitted
- [2] Hadrava P. (1995), “Orbital elements of multiple spectroscopic stars”, *A&AS* 114, 393
- [3] Hadrava P. (1997), “Relative line photometry of eclipsing binaries”, *A&AS* 122, 581
- [4] Hadrava P. (2001), “The method of spectra disentangling and its links to Doppler tomography” in: “Astrotomography, indirect imaging methods in observational astronomy”, eds. H.M.J. Boffin, D. Steeghs, J. Cuypers, *Lecture notes in physics* 573, 261
- [5] Hadrava P. (2004), “KOREL – User’s guide”, *Publ. Astron. Inst. ASCR* 92, 15
- [6] Hadrava P. (2006), “Disentangling of the spectra of binary stars – Principles, results and future development”, *Astrophys. & Sp. Sc.* 304, 337
- [7] Jingzhi Yan (2007), private communication
- [8] Karas V., Kraus P. (1996), “Doppler tomography of relativistic accretion disks”, *PASJ* 48, 771
- [9] Karitskaya E.A., Shimanskii V.V., Bochkarev N.G., Sakhbullin N.A., Galazutdinov G.A., Lee. B.-C. (2007), “Properties of the Cyg X-1 Optical Component”, *IAU Symp.* 240, 130
- [10] Sowers J.W., Gies D.R., Bagnuolo W.G., Jr., Shafter A.W., Wiemker R., Wiggs M.S. (1998), “Tomographic analysis of H $\alpha$  profiles in HDE 226868/Cygnus X-1”, *ApJ* 506, 424
- [11] Škoda P., Šlechta M. (2002), “Reduction of spectra exposed by the 700mm CCD camera of the Ondřejov telescope coudé spectrograph”, *Publ. Astron. Inst. ASCR* 90, 22